ACS Medicinal Chemistry Letters

pubs.acs.org/acsmedchemlett Letter

Covalent Bridging of Corilagin Improves Antiferroptosis Activity: Comparison with 1,3,6-Tri-*O*-galloyl-β-D-glucopyranose

Xican Li,* Jie Liu, Ban Chen, Yingci Chen, Wanjian Dai, Yuling Li, and Meiling Zhu*

Cite This: *ACS Med. Chem. Lett.* 2020, 11, 2232−2237 Read Online

ACCESS | Metrics & More | Article Recommendations | Supporting Information

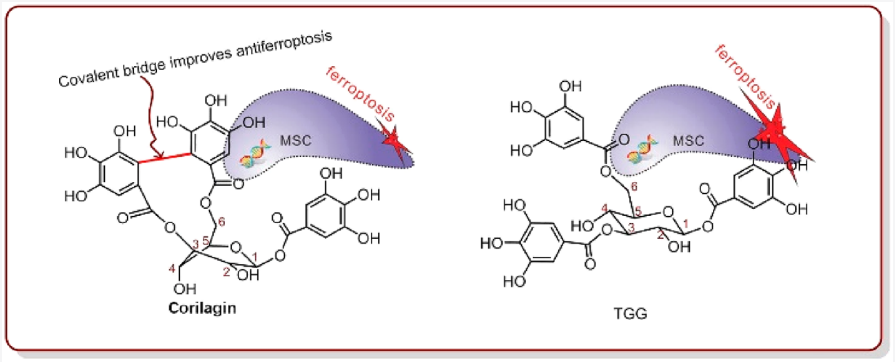

ABSTRACT: The ellagitannin corilagin and its analogue 1,3,6-tri-*O*-galloyl-β-D-glucopyranose (TGG) were found to protect bone marrow-derived mesenchymal stem cells (bmMSCs) against erastin-induced ferroptosis by cellular assays. However, the antiferroptosis bioactivity of corilagin was higher than that of TGG. Corilagin also exhibited higher antioxidant and Fe^{2+}-chelation levels than TGG. Treated with 1,1-diphenyl-2-picrylhydrazyl (DPPH) radicals, corilagin and TGG yielded a corilagin- and a TGG−DPPH adduct, respectively. The corilagin−DPPH adduct retained the covalent bridge throughout the ultrahigh-performance liquid chromatography coupled with electrospray ionization quadrupole time-of-flight tandem mass spectrometry (UHPLC-ESI-Q-TOF-MS) analysis. The strength of the covalent bridge is attributable to enhancement of its partial π−π conjugation. Thus, the bridge has sufficient strength to twist the chair conformation of the glucopyranosyl ring and to assemble two large aromatic rings, thereby improving the antioxidant (including Fe^{2+}-chelation) reactivities. The bridge can also stabilize the product intermediate via partial π−π conjugation. Hence, corilagin is a superior ferroptosis inhibitor and antioxidant compared to TGG.

KEYWORDS: *Corilagin, 1,3,6-tri-O-galloyl-β-D-glucopyranose, antiferroptosis, antioxidant, covalent bridging*

Nowadays, the search for novel ferroptosis inhibitors has become a hot issue. This is because the inhibition of ferroptosis can improve the availability of cellular transplantation engineering for treatment of ferroptosis-related diseases, e.g., neurodegenerative diseases.[1,2] Previously, natural radical scavengers (e.g., baicalein) have been indicated as potential ferroptosis inhibitors.[2,3] In addition, various Fe^{2+} chelators (e.g., deferoxamine) and metal-reducing reagents (e.g., β-mercaptoethanol) may also function as ferroptosis inhibitors.[3] Hence, ferroptosis can be inhibited through three pathways: radical scavenging, Fe^{2+}-chelation, and metal-reducing.

Based on this result, hydrolyzable tannins are presumed to be an important source of ferroptosis inhibitors because hydrolyzable tannins typically bear multiple galloyl groups and the galloyl group has strong radical scavenging, Fe^{2+}-chelation, and metal-reducing potential.[4,5] However, no evidence has been available to support this hypothesis. Since corilagin, a hydrolyzable tannin, has been suggested to have a potential for treating Parkinson's and Alzheimer's diseases,[6,7] we selected corilagin (Figure 1A, Figures S1−5, Supporting Information) and its analogue (TGG, Figure 1B, Figures S6−10, Supporting Information) as model compounds for the antiferroptosis investigation.

Early in 1951, corilagin was isolated from divi−divi (*Caesalpinia coriaria*);[8] later, it was found to coexist with TGG in *Terminalia chebula*.[7,9] Structurally, corilagin contains a covalent bridge between rings R_3 and R_6 (Figure 1). During hydrolysis, corilagin typically produces ellagic acid; thus, it is an ellagitannin, a subtype of hydrolyzable tannin.[10] In contrast to corilagin, TGG is merely a galloylglucose, which does not possess a corresponding covalent bridge.[11,12] Hence, the sole

Received: June 28, 2020
Accepted: October 2, 2020
Published: October 5, 2020

https://dx.doi.org/10.1021/acsmedchemlett.0c00359
ACS Med. Chem. Lett. 2020, 11, 2232−2237

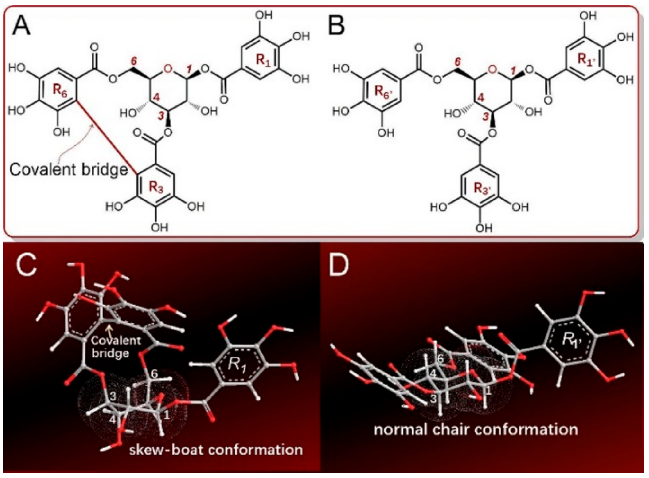

Figure 1. Structures and preferential conformation-based ball–stick models of corilagin and 1,3,6-tri-*O*-galloyl-*β*-D-glucopyranose (TGG). (A) Structure of corilagin; (B) structure of TGG; (C) a skew-boat conformation model of corilagin; (D) a normal chair conformation model of TGG. The energies of both corilagin and TGG were minimized with molecular mechanics II (MM2) using the Chem3D Pro14.0 program (PerkinElmer, Waltham, MA, USA) to create their preferential conformations.

difference between corilagin and TGG is the presence of an additional covalent bridge in corilagin, and the comparison between them can clarify whether this covalent bridge can regulate antiferroptosis in hydrolyzable tannins.

Undoubtedly, comparative studies will facilitate an understanding of the antiferroptosis and antioxidant chemistry of hydrolyzable tannins. Such understanding may further assist natural product chemists in the prediction of the relative antiferroptosis and antioxidant bioactivities between ellagitannins and their analogues (e.g., strictinin vs 1,4,6-tri-*O*-galloyl-*β*-D-glucopyranose, Figure S11, Supporting Information). For medicinal chemists, it may also provide important information for the design of effective ferroptosis inhibitors.

Previously, the bone marrow-derived mesenchymal stem cells (bmMSCs) have been reported to act as the seed cells in tissue transplantation for treatment of neurological disorders.[13−15] In this study, the bmMSCs were thus used as the model cells and treated with erastin, a small molecule. Erastin can inhibit the biosynthesis of glutathione (GSH), a cellular antioxidant, to impair redox balance that will trigger severe accumulation of LPO and other reactive oxygen species (e.g., $^{\bullet}O_2^-$), causing ferroptosis.[16,17] Thus, erastin has been used as a ferroptosis inducer in various cells including cancer cells.[18−20]

The bmMSCs in the erastin-treated group were analyzed using three cellular assays, including the 4,4-difluoro-5-(4-phenyl-1,3-butadienyl)-4-bora-3a,4a-diaz-s-indacen-3-undecanoic acid (C11-BODIPY) assay, cell counting kit-8 (CCK-8) assay, and flow cytometry assay. In the C11-BODIPY assay, the erastin-treated group displayed the darkest green color, implying that severe LPO accumulation occurred in cells (Figure 2A). Correspondingly, the erastin-treated group also showed the lowest cellular viabilities in the CCK-8 assay (Figure 2B) and in the flow cytometry assay (65.9%, Figure 2C). This supported the successful creation of an erastin-induced ferroptosis model in bmMSCs.

However, both the TGG and corilagin groups showed lighter green colors (Figure 2A) compared with the erastin group. This clearly indicated an LPO-inhibition effect in the TGG and corilagin groups. TGG presented darker green than corilagin, implying that corilagin was of a higher LPO-inhibition level than TGG.

A high LPO-inhibition level corresponds to a high cytoprotective level;[5] thus, corilagin was observed to exhibit higher cellular viability than TGG in the CCK-8 and flow cytometric assays (Figure 2C). In the flow cytometric assay, corilagin exhibited less early death (9.2%) and late death

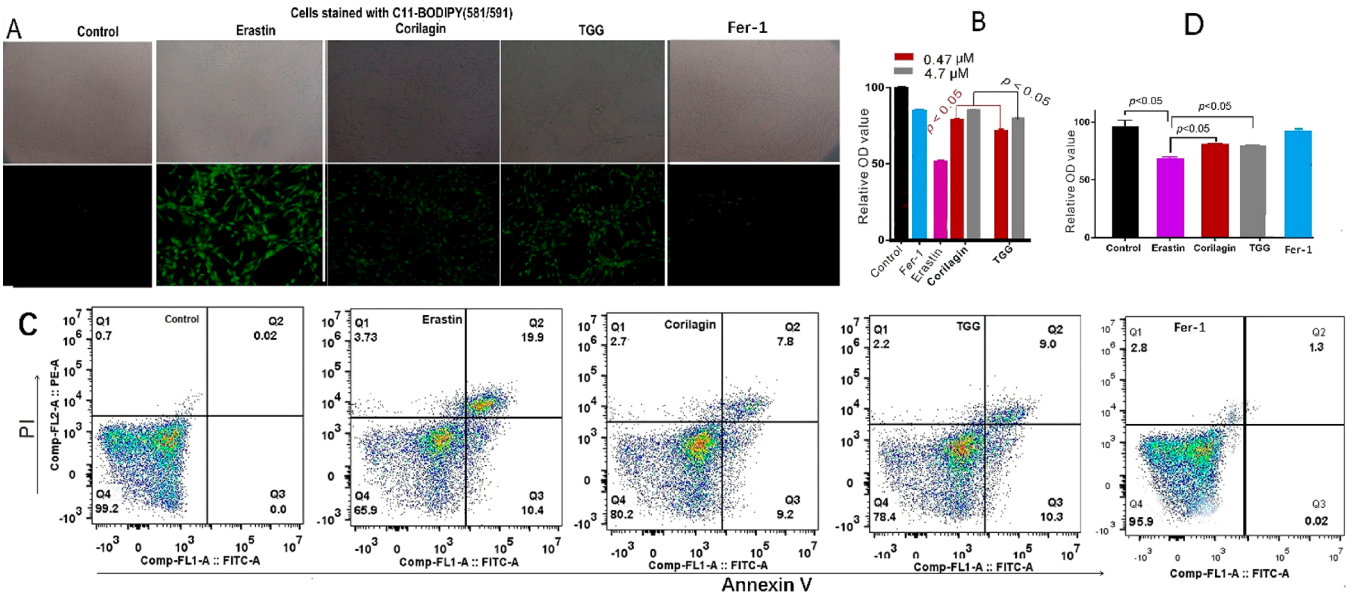

Figure 2. Preventive effects of corilagin and TGG on erastin-induced ferroptosis in bmMSCs: (A) the 4,4-difluoro-5-(4-phenyl-1,3-butadienyl)-4-bora-3a,4a-diaza-s-indacene-3-undecanoic acid (C11-BODIPY) assay; (B) the cell counting kit-8 (CCK-8) assay; (C) the flow cytometric assay; (D) the relative OD value characterizes the cell viability in flow cytometry (4.7 μM). In the C11-BODIPY assay, the green fluorescence indicates lipid peroxidation. In the CCK-8 assay, the value is expressed as mean ± SD (n = 3). In the flow cytometric assay, Q1, Q2, Q3, and Q4 correspond to the cellular death, late death, early death, and cellular viability, respectively. The concentration of Fer-1 (ferrostine-1) was 1 μM.

https://dx.doi.org/10.1021/acsmedchemlett.0c00359
ACS Med. Chem. Lett. 2020, 11, 2232−2237

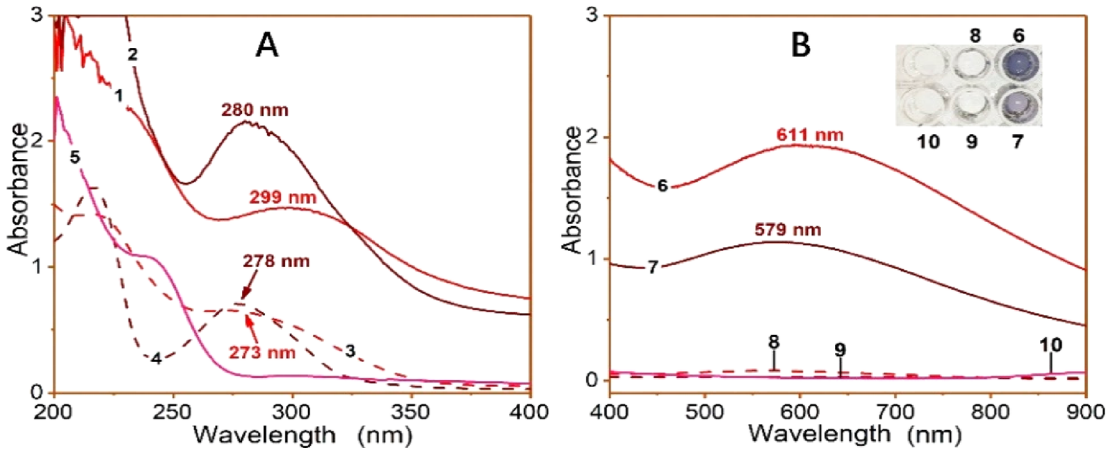

Figure 3. Experimental results of UV−vis spectra analysis of Fe^{2+}-chelation with corilagin and TGG: (A) the wavelength range of 200−400 nm; (B) the wavelength range of 400−900 nm; and (C) the appearance of the solutions (**1**, 0.25 mM corilagin plus 25 mM Fe^{2+}; **2**, 0.25 mM TGG plus 25 mM Fe^{2+}; **3**, 0.25 mM corilagin; **4**, 0.25 mM TGG; **5**, 25 mM Fe^{2+}; **6**, 0.50 mM corilagin plus 50 mM Fe^{2+}; **7**, 0.50 mM TGG plus 50 mM Fe^{2+}; **8**, 0.50 mM corilagin **9**, 0.50 mM TGG; **10**, 50 mM Fe^{2+}).

(7.8%) than TGG (10.3 and 9.0%, respectively); under the same conditions, the early death and late death of erastin were 10.4 and 19.9%, respectively (Figure 2C). Recently, ferroptosis has been reported to lead to neurological disorders;[21] hence, corilagin and TGG are expected to play roles in the prevention of neurological disorders.

As discussed above, Fe^{2+} plays a central role in ferroptosis; thus, Fe^{2+}-chelation may be the regulatory pathway for antiferroptosis or antioxidant bioactivities.[22,23] To explore the Fe^{2+}-chelation potential, both corilagin and TGG were respectively mixed with Fe^{2+} and then analyzed using UV−vis spectra and colorimetry.

In the UV−vis spectra, they produced corresponding red shifts (273 nm → 299 nm for corilagin and 278 nm → 280 nm for TGG) and strong shoulder peaks (611 nm and 576 nm, respectively). Meanwhile, the appearance of both corilagin and TGG solutions became darker (Figures 3A−B). In the colorimetry analysis, both corilagin and TGG showed good dose-dependent curves and lower IC_{50} values than sodium citrate, a metal chelator (Table 1 and Figure S12, Supporting Information). Therefore, the effectivity in Fe^{2+}-chelation assay implies that corilagin and TGG may utilize Fe^{2+}-chelation to exert their antiferroptosis actions.

Table 1. IC_{50} Values (μM) of Corilagin and TGG in Antioxidant Assays[a]

Assays	Corilagin	TGG	Trolox
Fe^{2+}-chelation	7 ± 1^{a}	11 ± 4^{b}	$14 \pm 2^{b,*}$
PTIO•-scavenging (pH 7.4)	94 ± 8^{a}	115 ± 11^{b}	445 ± 35^{c}
PTIO•-scavenging (pH 4.5)	204 ± 13^{a}	290 ± 35^{b}	289 ± 27^{b}
FRAP	12 ± 1^{a}	35 ± 2^{b}	81 ± 2^{c}
DPPH•-scavenging	1 ± 0^{a}	1 ± 0^{a}	7 ± 0^{b}

[a]The IC_{50} value (in μM unit) was defined as the final concentration of 50% radical inhibition or relative reducing/chelating power, which was calculated via linear regression analysis (Figures S12−16, Supporting Information) and expressed as the mean ± SD (n = 3). The linear regression was analyzed by the Origin 2017 professional software. The IC_{50} values with different superscripts (^{a}, ^{b}, or ^{c}) in the same row, differ significantly ($p < 0.05$). Trolox is the positive control (*denotes that the positive control is sodium citrate instead of Trolox). PTIO•, 2-phenyl-4,4,5,5-tetramethylimidazoline-1-oxyl 3-oxide radical; FRAP, Fe^{3+}-reducing antioxidant power; DPPH•, 1,1-diphenyl-2-picrylhydrazyl radical.

However, corilagin showed higher Fe^{2+}-chelation level than TGG (Figure 3 and Table 1). This may be due to their structural differences. Structurally, both corilagin and TGG are based on the glucopyranosyl moiety (Figure 1). The glucopyranosyl unit has various conformations, which include arrangements of the axial and equatorial bonds.[12,24] Previous theoretical chemistry studies and our molecular models that are based on MM2 calculation have identified the chair conformation as the preferred conformation of TGG, in which the $R_{1'}$, $R_{3'}$, and $R_{6'}$ rings are equatorially oriented and may extend in different directions (Figure 1D). However, in corilagin, the chair conformation is twisted because of the influence of the covalent bridge into a skew-boat preferred conformation (Figure 1C).[25,26] Through the conformation, corilagin can collaboratively chelate Fe^{2+} in the same direction. Thus, the covalent bridge strengthens the Fe^{2+}-chelation in corilagin.

To further probe the possible mechanisms, corilagin and TGG were evaluated using several antioxidant assays, including the 2-phenyl-4,4,5,5-tetramethylimidazoline-1-oxyl 3-oxide radical (PTIO•)-scavenging assay, the 1,1-diphenyl-2-picrylhydrazyl radical (DPPH•)-scavenging assay, and the Fe^{3+}-reducing antioxidant power (FRAP) assay. PTIO• is an oxygen-centered radical, while DPPH• is a nitrogen-centered radical.[27] In this study, the PTIO•-scavenging was assayed in aqueous solutions at pH 4.5 and 7.4, and the FRAP assay was conducted at pH 3.6 in aqueous solution, while the DPPH•-scavenging assay was conducted in an organic solvent.[26,27] In the three assays, both corilagin and TGG dose-dependently increased the antioxidant percentages and showed much lower IC_{50} values than the positive control, Trolox (Table1 and Figures S13−16 in the Supporting Information). Especially, in the DPPH•-scavenging assay, corilagin and TGG had 8- and 6.5-times lower IC_{50} values, respectively, than Trolox (Table 1). These data clearly demonstrate that both corilagin and TGG have significant antioxidant potential in organic and in aqueous solutions. This is consistent with previous findings.[28,29] Nevertheless, the relative antioxidant levels of corilagin and TGG differed. Corilagin always showed higher antioxidant levels than TGG in these assays (Table 1).

https://dx.doi.org/10.1021/acsmedchemlett.0c00359
ACS Med. Chem. Lett. 2020, 11, 2232−2237

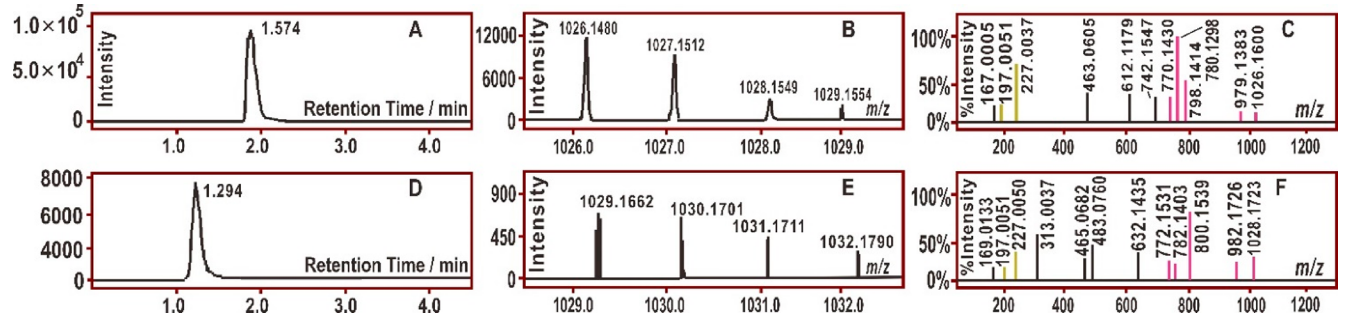

Figure 4. Typical results of the UHPLC-ESI-Q-TOF-MS analysis: (A) a chromatogram of the RAF product of the corilagin−DPPH adduct, from which the formula $[C_{45}H_{33}N_5O_{24}-H]^-$ was extracted; (B) the primary MS spectrum of the corilagin−DPPH adduct; (C) the secondary MS spectrum of the corilagin−DPPH adduct; (D) a chromatogram of the RAF product of the TGG−DPPH adduct, from which the formula $[C_{45}H_{35}N_5O_{24}-H]^-$ was extracted; (E) the primary MS spectrum of the TGG−DPPH adduct; (F) the secondary MS spectrum of TGG−DPPH adduct.

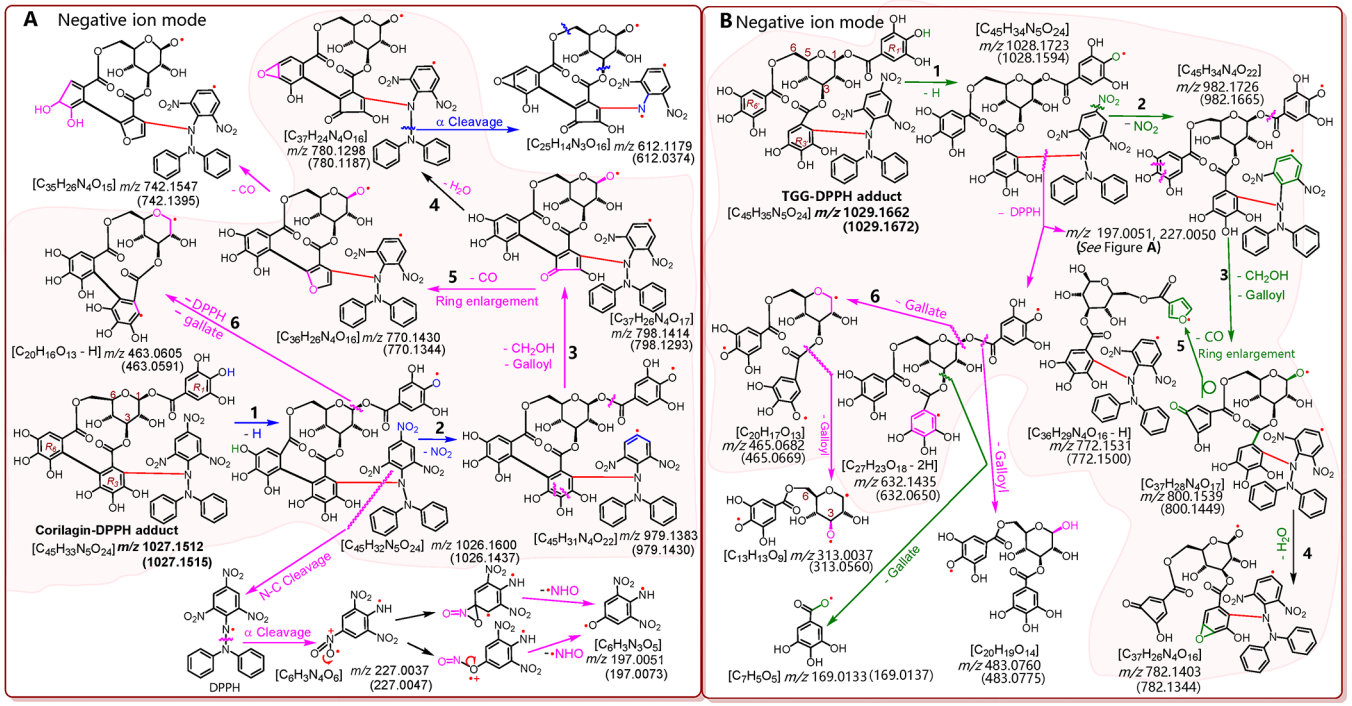

Figure 5. One of the possible structural and fragmentation pathways of corilagin−DPPH (A) and TGG−DPPH adducts (B). The accurate values in brackets are the m/z values that were calculated based on the relative atomic masses. The accurate m/z values without brackets are the experimental values that were obtained in the study. A comparison between the calculated and experimental values has demonstrated that no problem is encountered in the fragment composition. However, the fragment may be from other pathways, and DPPH may be attached to other positions. Nevertheless, this does not hinder the discussion. Other linking sites and other reasonable linkages and cleavages should not be excluded from the MS elucidation. The shaded pathways (**1**−**6**) are early fragmenting. The circle donates the rotation of the σ-bond.

Undoubtedly, the difference can also be attributed to the covalent bridge.

To determine the character of the covalent bridge, the reaction products of both corilagin and TGG with DPPH• were subjected to a UHPLC-ESI-Q-TOF-MS analysis. As shown in Figure 4A, the reaction of corilagin with DPPH• resulted in a chromatographic peak that corresponded to a molecular ion of m/z 1027.1512 (Figure 4B). The m/z value of 1027.1512 differed by one H atom (M.W. 1.007825) from the sum of the molecular weights of corilagin (M.W. 634.0806) and DPPH• (M.W. 394.0788).

The m/z value of 1027.1512 suggests the generation of a corilagin−DPPH adduct. This is because the m/z value had a relative deviation of 2.9×10^{-7} from the calculated molecular weight value (1027.1515 = 634.0806 + 394.0788). In the secondary MS data, the corilagin−DPPH adduct yielded two characteristic fragments (m/z 227.0037 and 197.0051, Figure 4C). The two characteristic fragments were reported to be from the DPPH unit (Figure 5).[30] The molecular ion and characteristic DPPH fragments permitted MS identification of the corilagin−DPPH adduct. A similar TGG−DPPH adduct has also been identified in the product mixtures of TGG and DPPH (Figures 4D−F).[30,31]

As shown in Figures 4 and 5, the molecular ion and six fragments (**1**−**6**) of the corilagin−DPPH adduct were parallel with those of the TGG−DPPH adduct. For example, corilagin−DPPH exhibited a fragment with m/z 1026.1600; correspondingly, TGG−DPPH gave a fragment with m/z 1028.1723. The m/z values of the former were two units less than those of the latter. The decrease of two m/z units

https://dx.doi.org/10.1021/acsmedchemlett.0c00359
ACS Med. Chem. Lett. 2020, 11, 2232−2237

corresponds to the presence of a covalent bridge in the corilagin adduct. As illustrated in Figure 5, even in the later MS fragmentations, the corilagin−DPPH adduct still retained the bridge. The presence of a covalent bridge in the whole MS fragmentations has clearly indicated its stability.

The stability of the bridge may be related to its linkage of two aromatic rings, namely, the $R_{3'}$ and $R_{6'}$ rings. The two rings are of steric hindrance. Once linked by a bridge, they may stagger to form a dihedral angle and present as partially planar. Through the partial planarity, they construct partial $\pi-\pi$ conjugation. Thus, the covalent bridge comprises a σ-bond and a partial π-bond. This is similar to the 3′,8″-linkage in isoginkgetin.[32]

The partial π-bond apparently reinforces the covalent bridge. Therefore, the bridge in corilagin possesses sufficient strength to twist the chair conformation of the glucopyranosyl ring into the skew conformation.[33,34] This conformation twist induces ring constraints, increasing the energy level of corilagin. Thus, corilagin had a higher $\triangle H^0_{f,0K}$ (formation heat) than TGG.[27] Similarly, our MM2 calculation suggested that the total energy of corilagin was elevated by 37.28 kcal/mol compared with that of TGG.[25] This elevated energy will activate the potential antioxidant reaction of corilagin. During the antioxidant reaction, corilagin probably donates a hydrogen atom at either the R_3 ring or the R_6 ring to produce an unstable product, a phenoxyl radical with an unpaired electron. However, the covalent bridge can delocalize the unpaired electron via partial $\pi-\pi$ conjugation, stabilizing the product intermediate.[26,27] The stabilization of the product intermediate can further facilitate hydrogen donation to improve the antioxidant levels of corilagin.

Now it is clear that the covalent bridge is seemingly connected by a σ-bond; however, it has a partial $\pi-\pi$ conjugation character. The conjugation can stabilize the product intermediate to promote the antioxidant action of corilagin. More importantly, the conjugation reinforces the covalent bridge. Thus, the bridge has sufficient strength to twist the glucopyranosyl ring into a skew conformation. Through the skew conformation, corilagin elevates the molecular energy and coordinates Fe^{2+}-chelation. Thus, corilagin demonstrates stronger antioxidant and antiferroptosis bioactivities than TGG.

In conclusion, ellagitannin corilagin and galloylglucose TGG can prevent bmMSCs from erastin-induced ferroptosis, possibly through their antioxidant-like activities, which include Fe^{2+}-chelation and direct radical scavenging. The covalent bridge carrying corilagin is superior to TGG in both antiferroptosis and antioxidant bioactivities, and the difference can only be attributed to the presence of the covalent bridge. The covalent bridge can twist glucopyranosyl ring conformation to cause cyclic restraint and assemble the aromatic rings to cause molecular crowding. In addition, it can also stabilize the product intermediate and collaboratively chelate Fe^{2+}. The high strength of the covalent bridge originates from the fact that the bridge is a σ bond with partial π character.

■ ASSOCIATED CONTENT

Supporting Information

The Supporting Information is available free of charge at https://pubs.acs.org/doi/10.1021/acsmedchemlett.0c00359.

Methods and materials; certificate of analysis of corilagin and 1,3,6-tri-*O*-galloyl-β-D-glucopyranose (TGG); typical covalent bridged ellagitannins and their analogues; dose response curves; MS elucidations (PDF)

■ AUTHOR INFORMATION

Corresponding Authors

Xican Li − *School of Chinese Herbal Medicine, Guangzhou University of Chinese Medicine, Guangzhou, People's Republic of China 510006*; orcid.org/0000-0002-4358-3993; Email: lixc@gzucm.edu.cn

Meiling Zhu − *Shenzhen Hospital of Integrated Traditional Chinese and Western Medicine, Shenzhen, People's Republic of China 518101*; Email: zml1930896811@163.com

Authors

Jie Liu − *Shenzhen Bao'an Traditional Chinese Medicine Hospital, Guangzhou University of Chinese Medicine, Shenzhen, People's Republic of China 518101*

Ban Chen − *School of Chinese Herbal Medicine, Guangzhou University of Chinese Medicine, Guangzhou, People's Republic of China 510006*

Yingci Chen − *School of Chinese Herbal Medicine, Guangzhou University of Chinese Medicine, Guangzhou, People's Republic of China 510006*

Wanjian Dai − *School of Chinese Herbal Medicine, Guangzhou University of Chinese Medicine, Guangzhou, People's Republic of China 510006*

Yuling Li − *School of Chinese Herbal Medicine, Guangzhou University of Chinese Medicine, Guangzhou, People's Republic of China 510006*

Complete contact information is available at: https://pubs.acs.org/10.1021/acsmedchemlett.0c00359

Author Contributions

The manuscript was written through contributions of all authors. All authors have given approval to the final version of the manuscript.

Funding

This research was funded by Nature Science Foundation of Guangdong Province (2017A050506043, 2017A030312009).

Notes

The authors declare no competing financial interest.

■ ABBREVIATIONS

bmMSCs, bone marrow-derived mesenchymal stem cells; C11-B ODIPY, 4,4-difluoro-5-(4-phenyl-1,3-butadienyl)-4-bora-3a,4a-diaza-s-indacene-3-undecanoic acid; CCK-8, cell counting kit-8; DPPH, 1,1-diphenyl-2-picrylhydrazyl radical; FRAP, Fe^{3+}-reducing antioxidant power; LPO, lipid peroxidation; PTIO, 2-phenyl-4,4,5,5-tetramethylimidazoline-1-oxyl 3-oxide radical; RAF, radical adduct formation; TGG, 1,3,6-tri-*O*-galloyl-β-D-glucopyranose; UHPLC-ESI-Q-TOF-MS, ultra-high-performance liquid chromatography coupled with electrospray ionization quadrupole time-of-flight tandem mass spectrometry; Fer-1, ferrostine-1.

■ REFERENCES

(1) Artyukhova, M. A.; Tyurina, Y. Y.; Chu, C. T.; Zharikova, T. M.; Bayir, H.; Kagan, V. E.; Timashev, P. S. Interrogating Parkinson's disease associated redox targets: potential application of CRISPR editing. *Free Radical Biol. Med.* **2019**, *144*, 279−292.

(2) Abdalkader, M.; Lampinen, R.; Kanninen, K. M.; Malm, T. M. R. Targeting Nrf2 to suppress ferroptosis and mitochondrial dysfunction in neurodegeneration. *Front. Neurosci.* **2018**, *12*, 466.
(3) Cong, L.; Dong, X.; Wang, Y.; Deng, Y.; Li, B.; Dai, R. On the role of synthesized hydroxylated chalcones as dual functional amyloid-β aggregation and ferroptosis inhibitors for potential treatment of Alzheimer's disease. *Eur. J. Med. Chem.* **2019**, *166*, 11−21.
(4) Serrano, J.; Puupponen-Pimia, R.; Dauer, A.; Aura, A.-M.; Saura-Calixto, F. Tannins: current knowledge of food sources, intake, bioavailability, and biological effects. *Mol. Nutr. Food Res.* **2009**, *53*, S310−S329.
(5) Kinoshita, S.; Inoue, Y.; Nakama, S.; Ichiba, T.; Aniya, Y. Antioxidant and hepatoprotective actions of medicinal herb, *Terminalia catappa* L. from Okinawa Island and its tannin corilagin. *Phytomedicine* **2007**, *14*, 755−762.
(6) Yanbing, D.; Lixia, H.; Jun, C.; Song, H.; Fahu, Y.; Jinwen, T. Corilagin attenuates the Parkinsonismin Japanese encephalitis virus induced Parkinsonism. *Transl. Neurosci.* **2018**, *9*, 13−16.
(7) Gaudreault, R.; Mousseau, N. Mitigating Alzheimer's disease with natural polyphenols: a review. *Curr. Alzheimer Res.* **2019**, *16*, 529−543.
(8) Li, X.; Deng, Y.; Zheng, Z.; Huang, W.; Chen, L.; Tong, Q.; Ming, Y. Corilagin, a promising medicinal herbal agent. *Biomed. Pharmacother.* **2018**, *99*, 43−50.
(9) Kim, M. S.; Lee, D. Y.; Lee, J.; Kim, H. W.; Sung, S. H.; Han, J. S.; Jeon, W. K. *Terminalia chebula* extract prevents scopolamine-induced amnesia *via* cholinergic modulation and anti-oxidative effects in mice. *BMC Complementary Altern. Med.* **2018**, *18*, 136.
(10) Yang, X.; Tomas-Barberan, F. A. Tea is a significant dietary source of ellagitannins and ellagic acid. *J. Agric. Food Chem.* **2019**, *67*, 5394−5404.
(11) Sylla, T.; Pouysegu, L.; Da Costa, G.; Deffieux, D.; Monti, J. P.; Quideau, S. Angew. Chem. Gallotannins and tannic Acid: first chemical syntheses and *in vitro* inhibitory activity on Alzheimer's amyloid β-peptide aggregation. *Angew. Chem., Int. Ed.* **2015**, *54*, 8217−8221.
(12) Ikuta, D.; Hirata, Y.; Wakamori, S.; Shimada, H.; Tomabechi, Y.; Kawasaki, Y.; Ikeuchi, K.; Hagimori, T.; Matsumoto, S.; Yamada, H. Conformationally supple glucose monomers enable synthesis of the smallest cyclodextrins. *Science* **2019**, *364*, 674−677.
(13) Volkman, R.; Offen, D. Concise review: mesenchymal stem cells in neurodegenerative diseases. *Stem Cells* **2017**, *35*, 1867−1880.
(14) Pisati, F.; Bossolasco, P.; Meregalli, M.; Cova, L.; Belicchi, M.; Gavina, M.; Marchesi, C.; Calzarossa, C.; Soligo, D.; Lambertenghi-Deliliers, G.; Bresolin, N.; Silani, V.; Torrente, Y.; Polli, E. Induction of neurotrophin expression via human adult mesenchymal stem cells: implication for cell therapy in neurodegenerative diseases. *Cell Transplant.* **2007**, *16*, 41−55.
(15) Malpass, K. Mesenchymal stem cells conditioned to secrete neurotrophic factors provide hope for Huntington disease. *Nat. Rev. Neurol.* **2012**, *8*, 120.
(16) D'Herde, K.; Krysko, D. V. Ferroptosis: oxidized PEs trigger death. *Nat. Chem. Biol.* **2017**, *13*, 4−5.
(17) Yang, W. S.; Kim, K. J.; Gaschler, M. M.; Patel, M.; Shchepinov, M. S.; Stockwell, B. R. Peroxidation of polyunsaturated fatty acids by lipoxygenases drives ferroptosis. *Proc. Natl. Acad. Sci. U. S. A.* **2016**, *113*, E4966−E4975.
(18) Doll, S.; Proneth, B.; Tyurina, Y. Y.; Panzilius, E.; Kobayashi, S.; Ingold, I.; Irmler, M.; Beckers, J.; Aichler, M.; Walch, A.; Prokisch, H.; Trumbach, D.; Mao, G.; Qu, F.; Bayir, H.; Fullekrug, J.; Scheel, C. H.; Wurst, W.; Schick, J. A.; Kagan, V. E.; Angeli, J. P.; Conrad, M. ACSL4 dictates ferroptosis sensitivity by shaping cellular lipid composition. *Nat. Chem. Biol.* **2017**, *13*, 91−98.
(19) Chen, Y.; Zhu, G.; Liu, Y.; Wu, Q.; Zhang, X.; Bian, Z.; Zhang, Y.; Pan, Q.; Sun, F. O-GlcNAcylated c-Jun antagonizes ferroptosis via inhibiting GSH synthesis in liver cancer. *Cell. Signalling* **2019**, *63*, 109384.
(20) Li, X. C. Improved pyrogallol autoxidation method: a reliable and cheap superoxide-scavenging assay suitable for all antioxidants. *J. Agric. Food Chem.* **2012**, *60*, 6418−6424.
(21) Wu, J. R.; Tuo, Q. Z.; Lei, P. Ferroptosis, a recent defined form of critical cell death in neurological disorders. *J. Mol. Neurosci.* **2018**, *66*, 197−206.
(22) Xie, Y.; Hou, W.; Song, X.; Yu, Y.; Huang, J.; Sun, X.; Kang, R.; Tang, D. Ferroptosis: process and function. *Cell Death Differ.* **2016**, *23*, 369−79.
(23) Gong, Y.; Wang, N.; Liu, N.; Dong, H. Lipid peroxidation and GPX4 inhibition are common causes for myofibroblast differentiation and ferroptosis. *DNA Cell Biol.* **2019**, *38*, 725−733.
(24) Staegemann, M. H. Conjugates of porphyrins and hyper-branched polyglycerol for an application in photodynamic therapy; Freie Universität Berlin Repository: Berlin, 2018; pp 373−381.
(25) Gaudreault, R.; van de Ven, T. G. M.; Whitehead, M. A. J. Mol. Model. Molecular modeling of poly (ethylene oxide) model cofactors:1,3,6-tri-*O*-galloyl-β-D-glucose and corilagin. *Molecular Modeling Annual* **2002**, *8*, 73−80.
(26) Li, X. C. 2-Phenyl-4,4,5,5-tetramethylimidazoline-1-oxyl 3-oxide (PTIO$^{\bullet}$) radical scavenging: a new and simple antioxidant assay *in vitro*. *J. Agric. Food Chem.* **2017**, *65*, 6288−6297.
(27) Li, X. Comparative study of 1,1-diphenyl-2-picryl-hydrazyl radical (DPPH$^{\bullet}$) scavenging capacity of the antioxidant xanthones family. *ChemistrySelect* **2018**, *3*, 13081−13086.
(28) Cho, E. J.; Yokozawa, T.; Rhyu, D. Y.; Kim, S. C.; Shibahara, N.; Park, J. C. Study on the inhibitory effects of Korean medicinal plants and their main compounds on the 1,1-diphenyl-2-picrylhydrazyl radical. *Phytomedicine* **2003**, *10*, 544−551.
(29) Hatano, T.; Yasuhara, T.; Yoshihara, R.; Agata, I.; Noro, T.; Okuda, T. Effects of interaction of tannins with co-existing substances. VII: inhibitory effects of tannins and related polyphenols on xanthine oxidase. *Chem. Pharm. Bull.* **1990**, *38*, 1224−1229.
(30) Ouyang, X.; Li, X.; Lu, W.; Zhao, X.; Chen, D. A null *B*-ring improves the antioxidant levels of flavonol: a comparative study between galangin and 3, 5, 7-trihydroxychromone. *Molecules* **2018**, *23*, 3083.
(31) Xie, Y.; Li, X.; Chen, J.; Deng, Y.; Lu, W.; Chen, D. pH Effect and chemical mechanisms of antioxidant higenamine. *Molecules* **2018**, *23*, 2176.
(32) Li, X.; Ouyang, X.; Cai, R.; Chen, D. 3′,8″-Dimerization enhances the antioxidant capacity of flavonoids: evidence from acacetin and isoginkgetin. *Molecules* **2019**, *24*, 2039.
(33) Karamat, S.; Fabian, W. M. Computational study of the conformational space of methyl 2,4-diacetyl-β-D-xylopyranoside: $^4C_1$ and $^1C_4$ chairs, skew-boats (^2S_O, $^1S_3$), and $B_{3,O}$ boat forms. *J. Phys. Chem. A* **2006**, *110*, 7477−7484.
(34) Li, X.; Wang, T.; Liu, J.; Liu, Y.; Zhang, J.; Lin, J.; Zhao, Z.; Chen, D. Effect and mechanism of wedelolactone as antioxidant-coumestan on $^{\bullet}$OH-treated mesenchymal stem cells. *Arabian J. Chem.* **2020**, *13*, 184−192.

https://dx.doi.org/10.1021/acsmedchemlett.0c00359
ACS Med. Chem. Lett. 2020, 11, 2232−2237